The Plant Cell, Vol. 24: 4483–4497, November 2012, www.plantcell.org © 2012 American Society of Plant Biologists. All rights reserved.

A Triantagonistic Basic Helix-Loop-Helix System Regulates Cell Elongation in *Arabidopsis*[W][OA]

Miho Ikeda,[a,b] Sumire Fujiwara,[a] Nobutaka Mitsuda,[a] and Masaru Ohme-Takagi [a,c,1]

[a] Bioproduction Research Institute, National Institute of Advanced Industrial Science and Technology, Tsukuba 305-8562, Japan
[b] Japanese Society for the Promotion of Science Chiyoda-ku, Tokyo 102-8472, Japan
[c] Institute for Environmental Science and Technology, Saitama University, Saitama 338-8770, Japan

In plants, basic helix-loop-helix (bHLH) transcription factors play important roles in the control of cell elongation. Two bHLH proteins, PACLOBTRAZOL RESISTANCE1 (PRE1) and *Arabidopsis* ILI1 binding bHLH1 (IBH1), antagonistically regulate cell elongation in response to brassinosteroid and gibberellin signaling, but the detailed molecular mechanisms by which these factors regulate cell elongation remain unclear. Here, we identify the bHLH transcriptional activators for cell elongation (ACEs) and demonstrate that PRE1, IBH1, and the ACEs constitute a triantagonistic bHLH system that competitively regulates cell elongation. In this system, the ACE bHLH transcription factors directly activate the expression of enzyme genes for cell elongation by interacting with their promoter regions. IBH1 negatively regulates cell elongation by interacting with the ACEs and thus interfering with their DNA binding. PRE1 interacts with IBH1 and counteracts the ability of IBH1 to affect ACEs. Therefore, PRE1 restores the transcriptional activity of ACEs, resulting in induction of cell elongation. The balance of triantagonistic bHLH proteins, ACEs, IBH1, and PRE1, might be important for determination of the size of plant cells. The expression of *IBH1* and *PRE1* is regulated by brassinosteroid, gibberellins, and developmental phase dependent factors, indicating that two phytohormones and phase-dependent signals are integrated by this triantagonistic bHLH system.

INTRODUCTION

In plants, regulation of cell elongation promotes proper growth and development, which includes cell differentiation, organ formation, patterning, and adaptation to environmental changes. Multiple phytohormones, namely, brassinosteroids (BRs), gibberellins (GAs), and auxin, positively regulate cell elongation throughout the plant life cycle (Depuydt and Hardtke, 2011). Plants also regulate cell elongation to respond to various environmental conditions, such as in shade avoidance. Far-red light and blue light positively and negatively regulate cell elongation, respectively (Briggs and Huala, 1999; Stamm and Kumar, 2010). However, the mechanism by which plants integrate multiple signals to regulate cell elongation has not been fully characterized.

In *Arabidopsis thaliana*, three atypical basic helix-loop-helix (bHLH) proteins of the PRE subfamily, PACLOBUTRAZOL RESISTANCE1 (PRE1), PRE3/ACTIVATION-TAGGED BRI1 SUPPRESSOR1 (PRE3/ATBS1), and PRE6/KIDARI (PRE6/KDR), positively regulate organ elongation in response to GA, BR, and light signaling, respectively (Hyun and Lee, 2006; Lee et al., 2006; Wang et al., 2009). PRE1 was first identified as a suppressor of the dwarf phenotype of the *ga2-201* mutant, which is defective in GA biosynthesis (Lee et al., 2006). The expression of *PRE1* is rapidly induced by GA treatment under the control of GIBBERELLIN INSENSITIVE, which is a negative regulator of GA signaling, indicating that GA regulates cell elongation by inducing the expression of *PRE1* (Lee et al., 2006).

By contrast, the rice (*Oryza sativa*) *PRE1* ortholog, *INCREASED LEAF INCLINATION1* (*ILI1*), acts in BR signaling; for example, ectopic expression of *ILI1* induced a BR-sensitive phenotype both in rice and *Arabidopsis* (Zhang et al., 2009). In *Arabidopsis*, the details of the BR signaling pathway are known: the Leu-rich repeat receptor-like kinase BRASSINOSTEROID-INSENSITIVE1 (BRI1) perceives BR at the cell surface and activates a phosphorylation-mediated signaling cascade (Li and Chory, 1997; Li, 2005) that activates the BRASSINAZOLE-RESISTANT1 (BZR1) and BZR2/BES1 transcription factors (Clouse, 2011). The BZR transcription factors regulate the expression of genes that are involved in cell wall biosynthesis and modification, namely, *XYLOGLUCAN ENDOTRANSGLUCOSYLASE/HYDROLASE* (*XTH*) and *EXPANSIN* (Rose et al., 2002; Li et al., 2003; Sun et al., 2010; Yu et al., 2011). BZR1 and BES1 and their rice orthologs, OsBZR1 and OsBES1, also activate the expression of *PRE1* and *ILI1*, respectively (Zhang et al., 2009; Sun et al., 2010).

ILI1 binding bHLH (IBH) protein and its *Arabidopsis* ortholog act as negative regulators of cell elongation and induce a dwarf phenotype when expressed ectopically (Zhang et al., 2009). BZR1 directly represses the expression of these genes by interacting with the promoter regions in the presence of BR (Zhang et al., 2009). The ectopic expression of *PRE1* suppressed the dwarf phenotype induced by the ectopic expression of *IBH1* (Zhang et al., 2009), showing that PRE1 inhibits the negative activity of IBH1 on cell elongation in response to GA and BR signaling.

PRE3/ATBS1 and PRE6/KDR, which belong to PRE subfamily, positively regulate organ elongation and interact with other bHLH proteins, including ATBS1-INTERACTING FACTORS

[1] Address correspondence to m-takagi@aist.go.jp.
The author responsible for distribution of materials integral to the findings presented in this article in accordance with the policy described in the Instructions for Authors (www.plantcell.org) is: Masaru Ohme-Takagi (m-takagi@aist.go.jp).
[W] Online version contains Web-only data.
[OA] Open Access articles can be viewed online without a subscription.
www.plantcell.org/cgi/doi/10.1105/tpc.112.105023

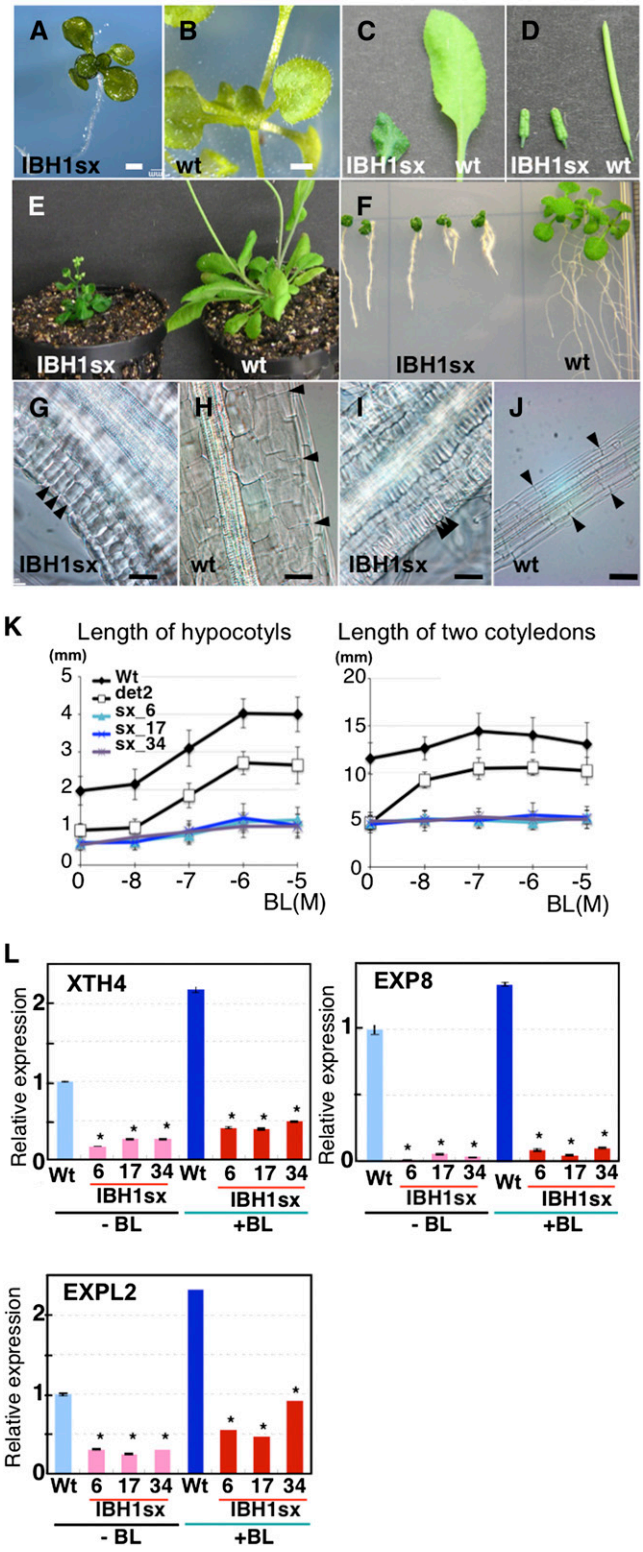

Figure 1. Analyses of *Pro35S:IBH1-SRDX* Plants.

(A) to **(F)** Seedlings (**[A]** and **[B]**), leaves **(C)**, siliques **(D)**, rosette plants **(E)**, and roots **(F)** of *Pro35S:IBH1-SRDX* plants (IBH1sx) and wild-type (wt) plants. Bars = 1 mm.

(AIFs) and LONG HYPOCOTYL IN FAR-RED1 (HFR1), which negatively regulate organ elongation (Hyun and Lee, 2006; Wang et al., 2009). The ectopic expression of *PRE6/KIDARI* suppressed the short hypocotyl phenotype induced by the ectopic expression of *HFR1* (Hyun and Lee, 2006), and the ectopic expression of *AIF1* suppressed the activity of PRE3/ATBS1 in BR-mediated organ elongation (Wang et al., 2009). These results indicate that PRE6/KDR and HFR1, PRE3/ATBS1 and AIFs, and PRE1 and IBH1 may antagonistically regulate organ elongation in their respective signaling pathways. Elongation of plant organs might be regulated by a pair of bHLH proteins composed of a PRE subfamily protein and its interacting bHLH protein, although the details of the regulatory mechanisms of cell elongation, including the functional role of PRE subfamily genes and the interacting bHLH, have yet to be revealed.

In this study, we show that *Arabidopsis* IBH1 interacts with other bHLH proteins that directly activate enzymatic genes for cell elongation. By interacting with these activators, IBH1 interferes with their activity, resulting in suppression of cell elongation. Furthermore, we show that IBH1 interference is interrupted by PRE1, which restores the transcriptional activity of the bHLH activators. We propose that cell elongation in plants is regulated by a system of competitive activities of triantagonistic bHLH proteins, including bHLH transcriptional activators and two atypical antagonistic bHLH inhibitors, and that the balance of each molecule is important for determination of the size of plant cells.

RESULTS

Arabidopsis Plants That Express a Chimeric IBH1 Repressor Are Insensitive to BRs

To identify transcription factors that regulate cell elongation in plants, we screened our set of transgenic *Arabidopsis* plants expressing chimeric repressor constructs (CRES-T lines). The CRES-T construct contains a transcription factor fused with the plant-specific repression domain derived from SUPERMAN (SUPERMAN REPRESSION DOMAIN X [SRDX]; LDLDLELRLGFA; Hiratsu et al., 2003) expressed under the control of the

(G) to **(J)** Micrograph of hypocotyls (**[G]** and **[H]**) and roots (**[I]** and **[J]**) of *Pro35S:IBH1-SRDX* plants (IBH1sx: **[G]** and **[I]**) and of wild-type plants (**[H]** and **[J]**). Black arrowheads indicate the borders of epidermal cells as an indication of cell size. Bars = 50 μm.

(K) Response of *Pro35S:IBH1-SRDX* plants to BR treatment. Length of hypocotyls (left) and two cotyledons (right) in the presence of different concentration of BL in 8-d-old seedlings of three independent lines of *Pro35S:IBH1-SRDX* (sx; light-blue line with triangle, blue line with X, and purple line with X), the wild type (black line), and *det2*-1 (black line with open square). Five-day-old seedlings grown on agar plates were transferred into liquid medium with or without BL and incubated for 3 d. Error bars indicate SD.

(L) qRT-PCR analyses of the *XTH4*, *EXP8*, and *EXPL2* genes in 10-d-old seedlings of the wild type (light-blue and blue bar) and three independent lines of *Pro35S:IBH1-SRDX* plants (IBH1sx; pink and red bars) with or without BL (10^{-7} M for 4 h) treatment. Asterisks indicate P values below 0.01 between the wild-type control and others.

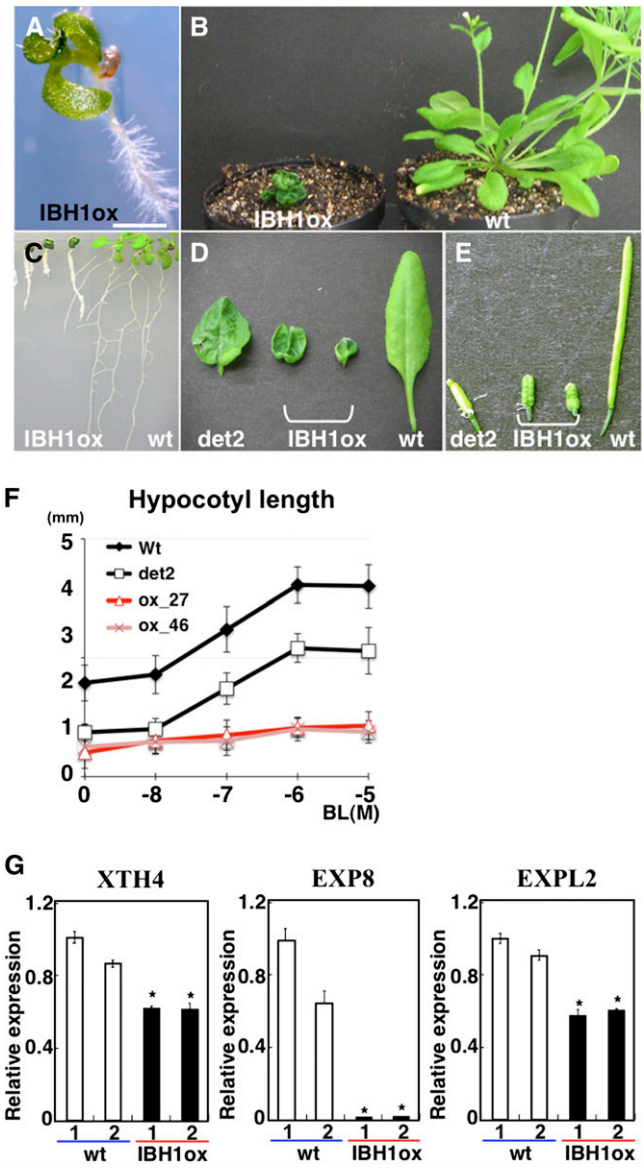

Figure 2. Analysis of *Pro35S:IBH1* Plants.

(A) to **(D)** Seedlings **(A)**, rosette plants **(B)**, roots **(C)**, leaves **(D)**, and siliques **(E)** of *Pro35S:IBH1* (IBH1ox), *det2* mutant (det2), and wild-type (wt) plants. Bar = 1 mm in **(A)**.

(F) Length of hypocotyls of the 8-d-old seedlings of two independent lines of *Pro35S:IBH1* (pink line with triangle and red line with X), wild-type (black line), and *det2*-1 (black line with open square) plants treated with different concentrations of BL ($n > 17$). Five-day-old seedlings grown on agar plates were transferred into liquid medium with or without BL and incubated for 3 d. Error bars indicate SD.

(G) qRT-PCR analyses of *XTH4*, *EXP8*, and *EXPL2* expression in two groups of 10-d-old seedlings of wild-type (open bars) and *Pro35S:IBH1* plants (IBH1ox; closed bars). Ten independent transgenic seedlings were mixed in each group. Asterisks indicate P values below 0.002 between wild-type 1 and others.

cauliflower mosaic virus (CaMV) 35S promoter. Fusion of the SRDX repression domain to a transcriptional activator can convert it into a strong repressor, which dominantly suppresses the expression of target genes. This overrides the activation by endogenous and functionally redundant transcription factors and results in a dominant-negative phenotype (Hiratsu et al., 2003). By contrast, the fusion of the SRDX to a native repressor enhances the repressive activity and induces a similar phenotype to its ectopic expression (Ikeda and Ohme-Takagi, 2009). We found that the CRES-T line for *At2g43060*, which was previously reported to be *Arabidopsis IBH1* (*Pro35S:IBH1-SRDX*), exhibited drastic dwarfism. *Pro35S:IBH1-SRDX* plants had round-shaped, dark-green leaves and short petioles, siliques, and roots, which had few lateral roots (Figures 1A to 1F). These phenotypes were similar to that of BR-insensitive mutants, such as *bri1* (Clouse et al., 1996; Clouse, 2011). These dwarf phenotypes appear to be specific to *Pro35S:IBH1-SRDX* plants because there were not observed in the CRES-T lines for other bHLHs, such as *Pro35S:HFR1-SRDX* (see Supplemental Figure 1A online). Also similar to BR-insensitive mutants, in the seedlings of *Pro35S:IBH1-SRDX* plants, elongation of hypocotyls in continuous dark conditions was decreased (see Supplemental Figure 1B online). Microscopy of hypocotyls and roots revealed that the dwarfism of *Pro35S:IBH1-SRDX* plants was due to reduced cell elongation (Figures 1G to 1J).

To determine whether the phenotypes of *Pro35S:IBH1-SRDX* plants were due to loss of sensitivity to BR or to defective BR biosynthesis, we treated seedlings with brassinolide (BL). When treated with BL, seedlings of wild-type plants and those of the BR biosynthesis defective mutant *det2* were pale green and had elongated hypocotyls and cotyledon petioles, although the elongation of hypocotyls of *det2* mutant plants was less than that of the wild type (Figures 1K; see Supplemental Figure 1C online). By contrast, seedlings of *Pro35S:IBH1-SRDX* plants did not exhibit this elongation response when treated with BL, indicating that the BR-insensitive phenotypes of *Pro35S:IBH1-SRDX* plants are due to loss of sensitivity to BR (Figures 1K; see Supplemental Figure 1C online).

Microarray analysis revealed that 13 genes for *XTH* and 14 genes for *EXP*, which are regulated by BR signaling, were downregulated in *Pro35S:IBH1-SRDX* plants (see Supplemental Table 1 online) (Sun et al., 2010; Yu et al., 2011). We confirmed the microarray results for some selected *XTH* and *EXP* genes, whose expression was less than fourfold in *Pro35S:IBH1-SRDX* plants when compared with wild-type plants in microarray analysis (see Supplemental Table 1 online). The results of quantitative RT-PCR (qRT-PCR) showed that *EXP8* levels were more than 20-fold lower and *XTH4* and *EXPL2* levels were more than threefold lower in *Pro35S:IBH1-SRDX* plants than in wild-type plants (Figure 1L). When plants were treated with BL, the levels of expression of those genes were upregulated in the wild type, but such upregulation was observed to be slight or nonexistent in the seedlings of *Pro35S:IBH1-SRDX* plants (Figure 1L). These results confirmed that *Pro35S:IBH1-SRDX* plants were insensitive to exogenous and endogenous BR and showed that IBH1 regulates BR-inducible genes.

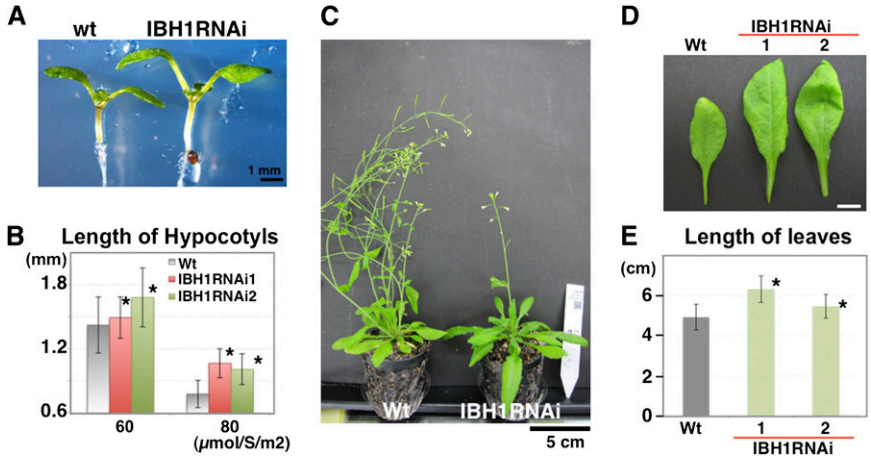

Figure 3. Analysis of *ProIBH1:IBH1RNAi* Plants.

(A) Seven-day-old seedlings of *ProIBH1:IBH1RNAi* (IBH1RNAi) and wild-type (wt) plants under 60 μmol/s/m^2. Bar = 1 mm.
(B) Analysis of length of hypocotyls of 7-d-old seedlings of two independent lines of *ProIBH1:IBH1RNAi* (IBH1RNAi; pink and green bar) and wild-type (gray bar) plants under 60 μmol/s/m^2 and 80 μmol/s/m^2. Asterisks indicate P values below 0.05 between the wild type and others. Error bars indicate SD (n > 89).
(C) Rosettes of *ProIBH1:IBH1RNAi* (IBH1RNAi) and wild-type plants. Bar = 5 cm.
(D) Leaves of 1.5-month-old *ProIBH1:IBH1RNAi* (IBH1RNAi) and wild-type plants. Bar = 1 cm.
(E) Analysis of length of leaves of two independent lines of *ProIBH1:IBH1RNAi* (IBH1RNAi; green bar) and wild-type (gray bar) plants. Asterisks indicate P values below 0.05 between the wild type and others. Error bars indicate SD (n > 15).

IBH1 Acts as a Transcriptional Repressor That Negatively Regulates BR Signaling and Cell Elongation

To further examine the function of IBH1 in BR signaling, we next made transgenic *Arabidopsis* that ectopically overexpressed *IBH1* (*Pro35S:IBH1*) (see Supplemental Figure 2A online). Zhang et al. (2009) reported that plants transformed with *Pro35S:IBH1* exhibited a dark-green and dwarf phenotype similar to *Pro35S:IBH1-SRDX* plants. We confirmed that our *Pro35S:IBH1* plants also exhibited the phenotype and insensitivity to BR similar to *bri1*, *det2*, and *Pro35S:IBH1-SRDX* plants (Figures 2A to 2F; see Supplemental Figure 2B online; Clouse, 2011). In addition, qRT-PCR analysis revealed that the expression of BR-inducible *EXPs* and *XTH4* in *Pro35S:IBH1* plants was downregulated (Figure 2G). These results indicated that the visible phenotype and the changes in gene regulation in *Pro35S:IBH1* plants were similar to those in *Pro35S:IBH1-SRDX* plants.

Usually, fusion of a transcriptional activator to SRDX phenocopies loss-of-function mutations of the transcription factor because the chimeric repressor dominantly suppresses target gene transcription (Hiratsu et al., 2003). By contrast, fusion of a native repressor to SRDX usually phenocopies ectopic expression of the transcription factor (Ikeda and Ohme-Takagi, 2009). The observation that *Pro35S:IBH1* and *Pro35S:IBH1-SRDX* plants exhibit similar phenotypes indicates that IBH1 acts as a transcriptional repressor.

We next examined the loss-of-function phenotype of *IBH1*. Because a T-DNA–tagged line for *IBH1* (*At2g43060*) was not available, we prepared transgenic plants that expressed an *IBH1* RNA interference (RNAi) under the control of the native *IBH1* promoter (*ProIBH1:IBH1RNAi*). We examined two independent RNAi lines in which the level of expression of *IBH1* was decreased to <25% of the wild type (see Supplemental Figure 3 online). These *ProIBH1:IBH1RNAi* plants were larger than the wild type (Figure 3C). Detailed phenotypic analysis revealed that the hypocotyls and leaves of *ProIBH1:IBH1RNAi* plants were significantly longer than those of the wild type (Figures 3A to 3E) and that the expression of *EXP8*, which was downregulated in *Pro35S:IBH1* and *Pro35S:IBH1-SRDX* plants, was upregulated in *ProIBH1:IBH1RNAi* plants (see Supplemental Figure 3 online). Because the phenotype of *ProIBH1:IBH1RNAi* was opposite to that of *Pro35S:IBH1-SRDX* and *Pro35S:IBH1*, our results indicate that IBH1 acts as a transcriptional repressor that negatively regulates BR signaling and organ elongation in *Arabidopsis*.

IBH1 May Be a Non-DNA Binding Transcriptional Repressor

To shed light on the mechanism of IBH1 function in cell elongation and gene expression, we next examined IBH1 for indications that it functions as a repressor. The IBH1 amino acid sequence does not contain any motif that can be categorized as a repression domain, such as an EAR motif, BRD, or WUS box (Ohta et al., 2001; Ikeda et al., 2009; Ikeda and Ohme-Takagi, 2009). Transient expression of the coding region of *IBH1* fused with the yeast GAL4 DNA binding domain (GAL4DB-IBH1) (Figure 4A) did not repress or activate a *Pro35S-GAL4:LUC* reporter gene in *Arabidopsis* leaves, but the GAL4DB-IBH1-SRDX (GAL4DB-IBH1sx) effector reduced the activity of the reporter gene to <20% (Figures 4A and 4B). These results indicate that *Arabidopsis* IBH1 does not have an active repressive activity but may instead act as a passive repressor.

Generally, passive repressors do not have direct repressive activity but instead may compete with other transcription factors for binding to a *cis*-element. To analyze whether IBH1 binds to

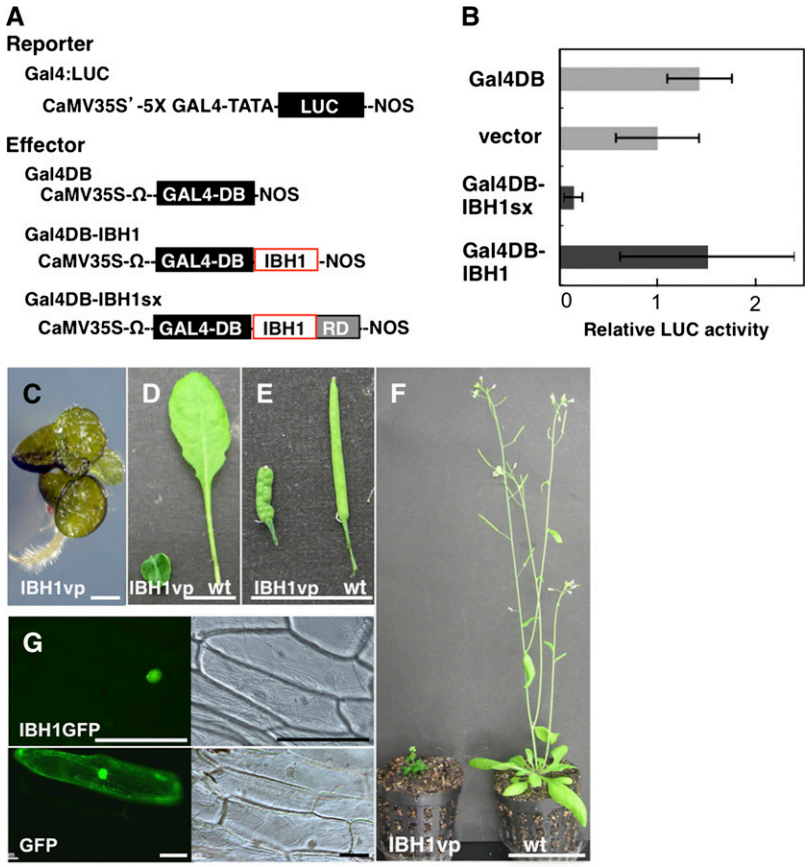

Figure 4. Analysis of the Molecular Function of IBH1.

(A) and **(B)** Transient expression assays for functional analysis of IBH1.

(A) Schematic representation of the constructs used in the transient expression analysis. The *Pro35S-GAL4:LUC* reporter gene (Gal4:LUC) contains the CaMV 35S promoter, five copies (5X) of the GAL4-responsive element, a minimal TATA region (−46 to transcription starting site of the CaMV 35S promoter), the firefly gene for luciferase (*LUC*; shown as a black box), and a nopaline synthase (NOS) terminator (Fujimoto et al., 2000). The effector constructs contain the protein coding region of *IBH1* (IBH; red open box) and *IBH1* with the SRDX repression domain (RD; gray box) fused to the GAL4 DNA binding domain (GAL4DB; black box), named Gal4DB-IBH1 and Gal4DB-IBH1sx. Each effector construct is driven by the CaMV 35S promoter and Ω translation enhancer sequence derived from *Tobacco mosaic virus*.

(B) Relative luciferase activities after cobombardment of *Arabidopsis* leaves with GAL4DB-fused *IBH1* effectors and the GAL4:LUC reporter gene. The relative activity due to pUC18 vector (vector) was set as 1. Error bars indicate SD (n = 3).

(C) to **(F)** Phenotypic analysis of *Pro35S:IBH1-VP16* plants. A seedling **(C)**, leaves **(D)**, siliques **(E)**, and a rosette plant **(F)** of *Pro35S:IBH1-VP16* (AtIBH1vp) and wild-type (wt) plants. Bars = 1 mm in **(C)**, 1 cm in **(D)** and **(E)**, and 5 cm in **(F)**.

(G) Nuclear localization of IBH1 fused with GFP (IBH1GFP; top two panels). Bottom two panels are control GFP. Bar = 100 μm.

DNA, we prepared transgenic plants that expressed *IBH1* fused with the VP16 activation domain (*Pro35S:IBH1-VP16*). The VP16 activator domain should activate the expression of a target gene if it interacts with DNA through IBH1, resulting in a phenotype opposite to *Pro35S:IBH1-SRDX* plants. Interestingly, however, *Pro35S:IBH1-VP16* plants exhibited a similar phenotype to that of *Pro35S:IBH1* and *Pro35S:IBH1-SRDX* plants, namely, round-shaped, dark-green leaves and short hypocotyls (Figures 4C to 4F). These results indicate that the VP16 activation domain did not affect the repressive activity of IBH1 and that IBH1 may not bind to DNA, directly or indirectly.

Toledo-Ortiz et al. (2003) reported that the Glu-13 and Arg-17 amino acids in the basic motif of bHLH proteins are necessary for binding to the E-box (CAGCTG) and G-box (CACGTG), which are the typical binding sequences of bHLH proteins. Our amino acid comparison showed that the bHLH region of IBH1 was clearly diverged from that of typical bHLH proteins and lacks the amino acid necessary for binding to the E-box and G-box in the basic motif (see Supplemental Figure 4 online). These analyses also support that IBH1 may not have DNA binding activity. One of the typical non-DNA binding HLH proteins, human Inhibitor of DNA binding 1 (Id-1), has been shown to inhibit the activity of other bHLH transcription factors by heterodimerization (Ruzinova and Benezra, 2003). Because IBH1 localizes to the nucleus, as was shown using an IBH1-GFP (for green fluorescent protein) fusion protein (Figure 4G), we hypothesized that IBH1 may interfere, possibly through physical interaction, with the DNA binding activity of other transcription factors that activate cell elongation.

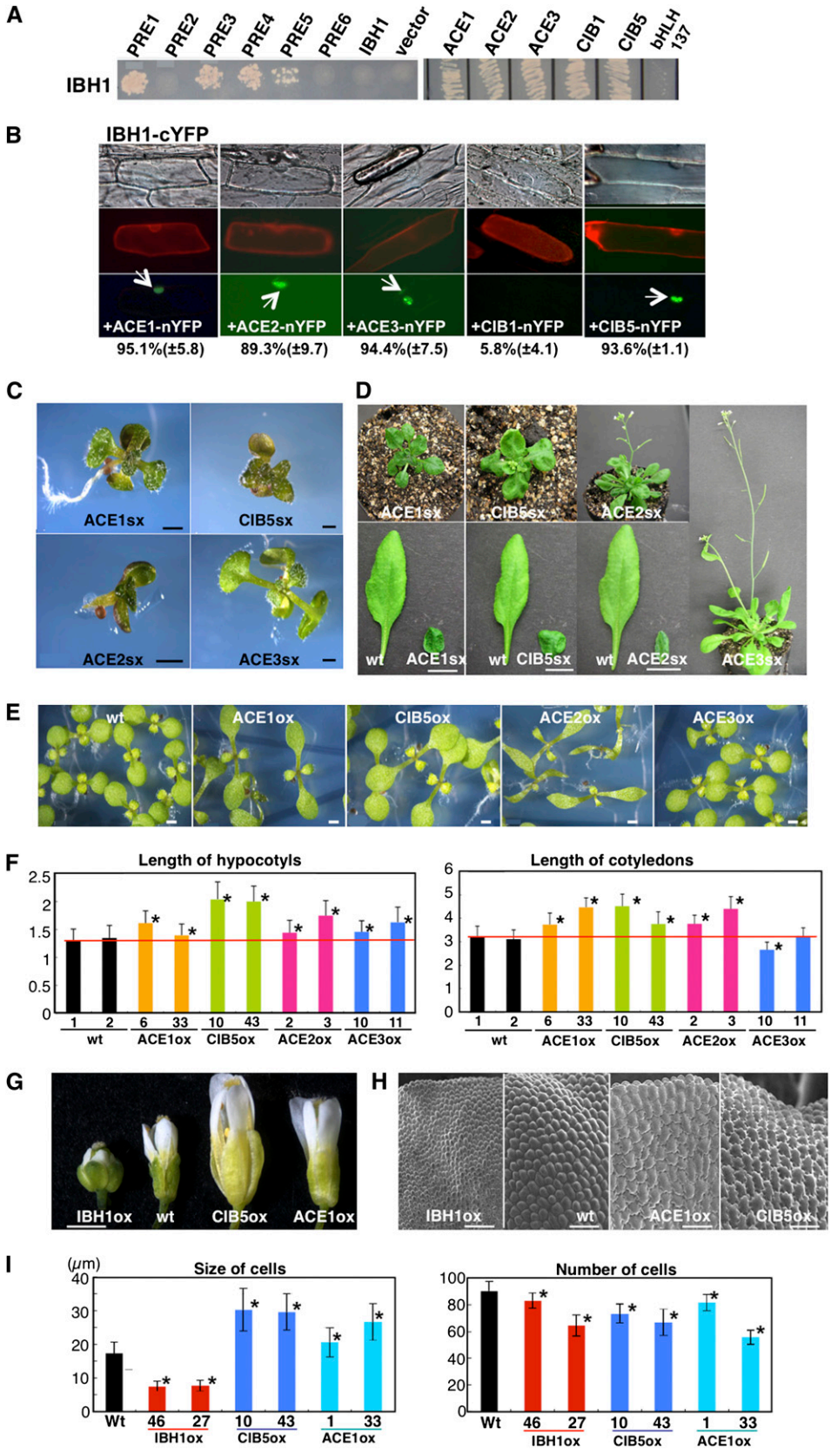

Figure 5. Analysis of transcription Factors That Interact with IBH1.

bHLH Transcription Factors That Interact with IBH1

We predicted that IBH1 interacts with, and thus interferes with, the activity of transcription factors that activate the genes required for cell elongation. To identify those factors that interact with IBH1, we next performed yeast two-hybrid (Y2H) screens using our cDNA library composed of only *Arabidopsis* cDNAs for transcription factors (Mitsuda et al., 2010). Among 22 positive clones isolated, 16 encode typical bHLH transcription factors, including bHLH049 (*At1g68920*), bHLH074 (*At1g10120*), and bHLH077 (*At3g23690*) (see Supplemental Table 2 online). In addition, we found that IBH1 interacted with PRE1, confirming a previous report that PRE1 interacts with IBH1 (Zhang et al., 2009). We also found that IBH1 interacted with several PRE subfamily proteins, namely, PRE3, PRE4, and PRE5, by individual Y2H assay (Figure 5A; see Supplemental Table 2, Supplemental Figure 5, and Supplemental Data Set 1 online).

Phylogenetic analysis showed that bHLH049, bHLH074, and bHLH077 are classified into the same subfamily of bHLH transcription factors (Heim et al., 2003; Toledo-Ortiz et al., 2003). We analyzed the interaction between IBH1 and each of those 12 bHLHs by individual Y2H assays and found that CRYPTOCHROME INTERACTING BASIC-HELIX-LOOP-HELIX1 (CIB1) and CIB5 (Liu et al., 2008) also interacted with IBH1 in yeast, as did bHLH049, bHLH074, and bHLH077 (Figure 5A). We also analyzed the interaction of IBH1 with those bHLHs in plant cells using bimolecular fluorescence complementation (BiFC) in transient expression experiments using onion epidermal cells. The BiFC analyses revealed that bHLH049, bHLH074, bHLH077, and CIB5 were capable of forming a heterodimer with IBH1 in the nucleus, but CIB1 did not (Figure 5B; see Supplemental Figure 6A online). We named bHLH049, bHLH074, and bHLH077 as ACTIVATOR FOR CELL ELONGATION1 (ACE1) to ACE3 (see Supplemental Figure 5 and Supplemental Data Set 1 online).

ACEs Act as Transcriptional Activators for Cell Elongation

To analyze the biological functions of the *ACEs* and *CIB5* genes, we prepared transgenic *Arabidopsis* plants that express chimeric repressor constructs for each of the ACEs and CIB5 (*Pro35S*:*ACE1-SRDX*, *Pro35S*:*ACE2-SRDX*, *Pro35S*:*ACE3-SRDX*, and *Pro35S*:*CIB5-SRDX*). Results showed that *Pro35S*:*ACE1-SRDX*, *Pro35S*:*ACE2-SRDX*, and *Pro35S*:*CIB5-SRDX* transgenic plants had dwarf stature, round-shaped, dark-green leaves and short siliques, which was similar to the phenotypes of *Pro35S*:*IBH1* and *Pro35S*:*IBH1-SRDX* plants; by contrast, *Pro35S*:*ACE3-SRDX* plants had a phenotype similar to the wild type (Figures 5C and 5D).

In contrast with the chimeric repressor phenotypes, seedlings of transgenic *Arabidopsis* that ectopically expressed each *ACE1-3* and *CIB5* (*Pro35S*:*ACE1*, *Pro35S*:*ACE2*, *Pro35S*:*ACE3*, and *Pro35S*:*CIB5*) had slightly but significantly longer hypocotyls than wild-type plants (Figure 5F). The cotyledons of the seedlings of *Pro35S*:*ACE1*, *Pro35S*:*ACE2*, and *Pro35S*:*CIB5* plants were slender, pale green, and longer than the wild type, phenotypes opposite to that of *Pro35S*:*AtIBH1* and *Pro35S*:*AtIBH1-SRDX* plants, and those of *Pro35S*:*ACE3* plants were similar or slightly shorter than those of the wild type (Figures 5E and 5F). In rosette plants, flowers, petals, and sepals of *Pro35S*:*ACE1* and *Pro35S*:*CIB5* plants were larger than the wild-type, but *Pro35S*:*IBH1* plants had much smaller flowers than the wild type (Figure 5G). Detailed morphological analysis using scanning electron microscopy revealed that the larger size of petals of *Pro35S*:*ACE1* and *Pro35S*:*CIB5* plants was due to increased cell length but not to increased cell number (Figures 5H and 5I). These results indicated that ACE1, ACE2, and CIB5 act as transcriptional activators that positively regulate cell elongation, although the activity of ACE3 seemed to be weaker than the others.

ACE1 Binds to the G-Box and IBH1 Inhibits Its Binding Activity

To analyze whether IBH1 interferes with the activity of ACEs, we performed transient expression assays using a reporter construct in which four tandem repeats of CIB binding element (CIBE), which was reported to be a binding element for CIB1 (see Supplemental Table 3 online; Liu et al., 2008) and contains a G-box (Liu et al., 2008), were placed upstream of a LUC reporter gene (*CIBE4*:*LUC*; Figure 6A). Results of transient expression assays showed that the activity of the *CIBE4*:*LUC*

Figure 5. (continued).

(A) Interaction between IBH1 and PRE subfamily, ACEs, and CIBs in Y2H assay on -L-H medium using IBH1 as bait.

(B) BiFC assay for the detection of interaction between bHLHs and IBH1 in onion epidermal cells. Percentage of cells in which bright green fluorescence was observed in the nucleus is shown. Numbers in parentheses indicate SD ($n \geq 100$). Arrows indicate bright green fluorescence.

(C) and **(D)** Phenotypic analysis of *Pro35S*:*ACE-SRDX* plants and *Pro35S*:*CIB5-SRDX* plants. Seven-day-old seedlings **(C)** and rosette plant and leaves **(D)** that ectopically expressed the chimeric repressor gene for each of the three ACEs and CIB5 (*Pro35S*:*ACE1-SRDX*; ACE1sx, *Pro35S*:*ACE2-SRDX*; ACE2sx, *Pro35S*:*ACE3-SRDX*; ACE3sx, *Pro35S*:*CIB5-SRDX*; CIB5sx), respectively. Bar = 1 mm in **(C)** and 1cm in **(D)**.

(E) to **(I)** Analysis of *Pro35S*:*ACE* plants.

(E) Seven-day-old seedlings that ectopically expressed each of the three ACEs and CIB5 (*Pro35S*:*ACE1*; ACE1ox, *Pro35S*:*ACE2*; ACE2ox, *Pro35S*:*ACE3*; ACE3ox, *Pro35S*:*CIB5*; CIB5ox), respectively. Bar = 1 mm.

(F) Analysis of length of hypocotyls (left) and of cotyledons (right) of 7-d-old seedlings that ectopically expressed the ACEs and CIB5 and wild-type (wt) plants. Asterisks indicate P values below 0.05 between the wild type and others. Error bars indicate SD ($n > 42$).

(G) and **(H)** Flowers **(G)** and electron micrographs of the abaxial sides of petals **(H)** of flowers of *Pro35S*:*IBH1* (AtIBH1ox), *Pro35S*:*ACE1* (ACE1ox), *Pro35S*:*CIB5* (CIB5ox), and wild-type plants. Bar = 1 mm in **(G)** and 50 μm in **(H)**.

(I) Length of cells of the top part of a petal (left panel) and number of cells in the lines of a petal from bottom to top (right panel) in *Pro35S*:*ACE1* (ACE1ox), *Pro35S*:*CIB5* (CIB5ox), *Pro35S*:*IBH1* (IBH1ox), and wild-type flowers. Asterisks indicate P values below 0.05 between the wild type and others. Error bars indicate SD ($n = 50$ in left panel and 6 in right panel).

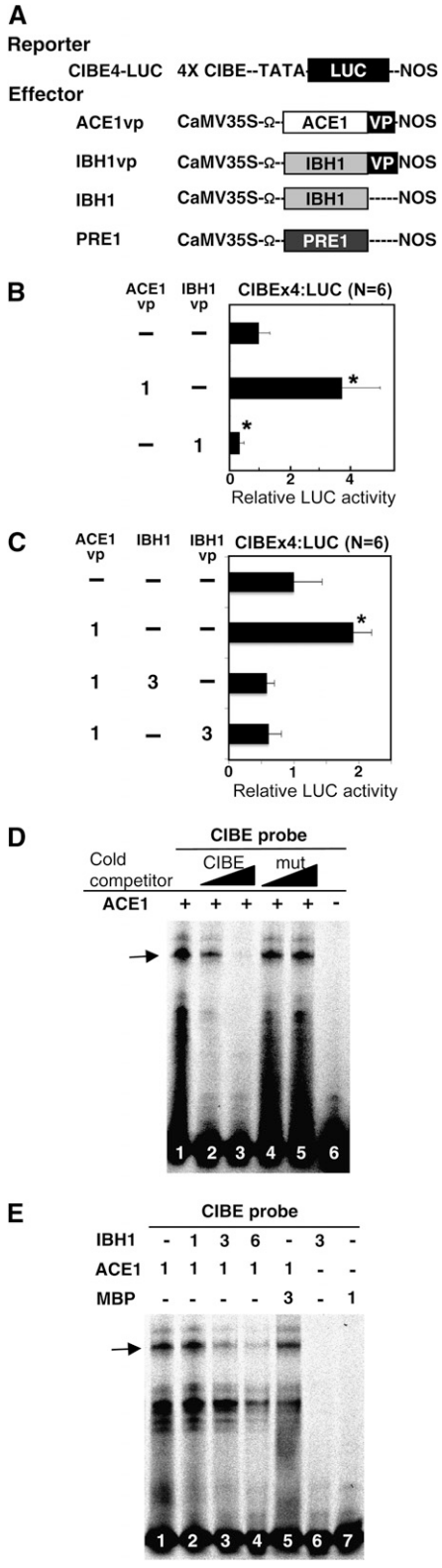

Figure 6. IBH1 Inhibits the Binding of ACE1 to CIBE.

(A) Schematic representation of the constructs used in transient expression analysis. *CIBEx4:LUC* reporter gene, which contained four copies of the CIB binding element (4xCIBE; see Supplemental Table 3 online), fused upstream of the LUC gene (LUC; shown as a black box) (Fujimoto et al., 2000) and the effector constructs for ACE1 (open box) fused with the VP16 activation domain (vp; shown as a black box) (ACE1vp), IBH1, IBH1 (gray box) fused with VP16 activation domain (IBH1vp), IBH1 (IBH1) and PRE1 (PRE1), driven by the CaMV 35S promoter are shown. Ω, translational enhancer sequence derived from *Tobacco mosaic virus*.

(B) and **(C)** Suppression of the activity of ACE1 by IBH1. Relative luciferase activities after cobombardment of *Arabidopsis* leaves with ACE1vp, IBH1, and IBH1vp effectors, respectively, and the *CIBEx4:LUC* reporter gene. The relative activity due to vector control (top bar) was set as 1. Error bars indicate SD. Asterisks indicate P values below 0.05 between vector control and others. Numbers indicate the ratio of effector construct (1 = 0.3 μg for one experiment).

(D) and **(E)** IBH1 inhibited the binding of ACE1 protein to the CIBE probe. EMSAs were performed using ACE1, IBH1, and MBP proteins, which were produced in *Escherichia coli.* MBP was used as a control protein. The CIBE probe (all lanes) was incubated with ACE1 protein (lanes 1 to 5 in **[D]** and lanes 1 to 5 in **[E]**), IBH1 (lane 2 to 4 and 6 in **[E]**) and MBP (lane 6 in **[D]** and lanes 5 and 7 in **[E]**). Unlabeled CIBE probe (CIBE; lanes 2 and 3 in **[D]**) and mutated CIBE probe (mut; lanes 4 and 5 in **[D]**) were used as cold competitor DNA. Numbers indicate the ratio of protein (1 = 0.6 μg for one lane). The arrow indicates the specific ACE1-DNA complex.

reporter gene was upregulated severalfold when the *Pro35S:ACE1-VP16* (ACE1vp) effector, in which the VP16 activation domain was fused with the C terminus of ACE1, was coexpressed (Figures 6A and 6B), showing that ACE1 bound to CIBE. By contrast, when the *Pro35S:IBH1-VP16* (IBH1vp) effector was coexpressed with the *CIBE4:LUC* reporter gene, the reporter gene was not activated, indicating that IBH1 did not bind to CIBE either directly or indirectly (Figure 6B).

When the *CIBE4:LUC* reporter was transiently transformed along with *Pro35S:IBH1* (IBH1) and ACE1vp effectors, the activation of the *CIBE4:LUC* reporter gene was suppressed to the basal level (Figure 6C). In addition, the IBH1vp effector was also able to suppress ACE1vp effector activation of the *CIBE4:LUC* reporter gene (Figure 6C). These results indicated that IBH1, with or without the VP16 activation domain, inhibited the transcriptional activation activity of the ACE1vp effector and that IBH1 did not compete with ACE1 for binding to CIBE but might interfere with ability of ACE1 to bind to CIBE.

The ability of IBH1 to interfere with the DNA binding activity of ACE1 was confirmed by electrophoresis mobility shift assay (EMSA). EMSA results showed that ACE1 protein specifically bound to the CIBE fragment but did not bind to a mutated CIBE fragment (Figure 6D). When IBH1 protein was added to the ACE1-CIBE complex mixture, the complex was destroyed in a dose-dependent manner (Figure 6E). The EMSA data also confirmed that IBH1 did not bind to the CIBE fragment (Figure 6E).

In addition, immunoprecipitation assays clearly showed heterodimer formation between ACE1 and IBH1 in *Nicotiana benthamiana* cells (Figures 7A and 7D), confirming the Y2H assay and BiFC assays in onion epidermal cells (Figures 5A and 5B; see Supplemental Figure 6A online). These results indicate that IBH1 very likely inhibits the DNA binding of ACE1 to the CIBE fragment by forming a heterodimer with ACE1.

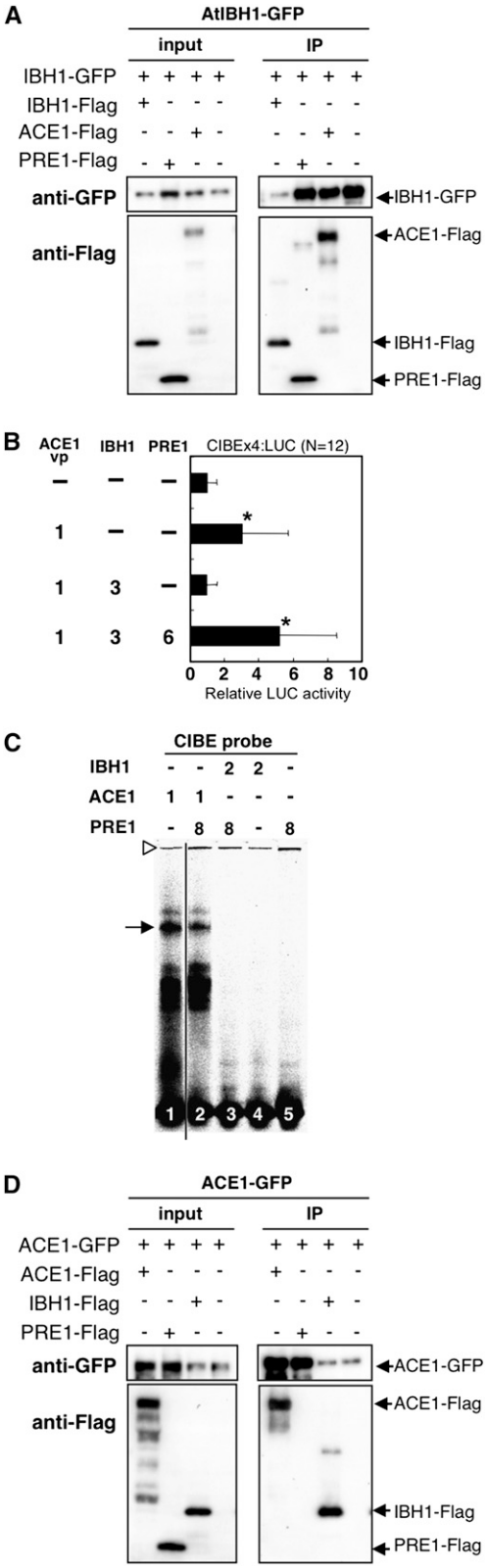

Figure 7. PRE1 Restores Activity of ACE1 by Interfering with Negative Activity of IBH1.

(A) Coimmunoprecipitation of IBH1 with PRE1 and ACE1 in vivo. IBH1-GFP with IBH1-Flag, PRE1-Flag, and ACE1-Flag were transiently coexpressed in *N. benthamiana*. IBH1-GFP was detected by anti-GFP and IBH1-Flag, and PRE1-Flag and ACE1-Flag were detected by anti-Flag antibodies. Blots are representative of multiple trials.

(B) Relative luciferase activities after cobombardment of *Arabidopsis* leaves with ACE1vp, IBH1, and PRE1 effectors and the *CIBEx4*:*LUC* reporter gene. The relative activity due to vector control (top bar) was set as 1. Error bars indicate SD (n = 12). Asterisks indicate P values below 0.05 between vector control and others. Numbers indicate the ratio of effector construct (1 = 0.3 μg for one experiment).

(C) EMSA performed using ACE1, IBH1, and PRE1 proteins, which were produced in *E. coli.* The CIBE probe (all lanes) was incubated with ACE1 (lanes 1 and 2), IBH1 (lanes 3 and 4) and PRE1 (lanes 2, 3, and 5). Numbers indicate the ratio of protein (1 = 0.6 μg for one lane). The arrow indicates the specific ACE1-DNA complex. Open triangle indicates the loading well.

(D) Coimmunoprecipitation of ACE1 with PRE1 and IBH1 in vivo. ACE1-GFP with IBH1-Flag, PRE1-Flag, and ACE1-Flag was transiently c-expressed in *N. benthamiana*. ACE1-GFP was detected by anti-GFP and IBH1-Flag, and PRE1-Flag and ACE1-Flag were detected by anti-Flag antibodies. Blots are representative of multiple trials.

PRE1 Interferes with the Negative Activity of IBH1 on ACE1

PRE1 was previously reported to act as a positive regulator of plant cell elongation and to interact with IBH1 (Lee et al., 2006; Zhang et al., 2009). We confirmed the interaction of PRE1 with IBH1 in our Y2H and BiFC assays (Figures 5A and 5B; see Supplemental Figure 6 online). In addition, our immunoprecipitation assays showed an in vivo interaction between IBH1 and PRE1 (Figure 7A). Then, we hypothesized that PRE1 induced cell elongation by interfering with the negative activity of IBH1 on the ACEs.

To test our hypothesis that PRE1 suppresses the negative activity of IBH1 on ACEs, we performed transient expression assays. The upregulation of the *CIBE4*:*LUC* reporter gene by ACE1vp effector was suppressed when IBH1 was coexpressed. However, the upregulation of *CIBE4*:*LUC* activity was restored when PRE1 was coexpressed with IBH1 and ACE1 (Figure 7B). Therefore, PRE1 was able to counteract the negative effect of IBH1. These results indicate that PRE1 interfered with the negative activity of IBH1 on ACE1.

In addition, EMSA assays showed that IBH1, PRE1, or the PRE1-IBH1 complex did not bind to the CIBE fragment and that PRE1 protein did not supershift the ACE1-CIBE complex (Figure 7C). These results indicate that IBH1 and PRE1 do not have DNA binding activity to CIBE fragment and PRE1 did not interact with the ACE1-CIBE complex. Moreover, we did not detect interaction between PRE1 and ACE1 in either BiFC or immunoprecipitation assays where interaction of ACE1 and IBH1 was clearly observed (Figure 7D; see Supplemental Figure 6B online). These results indicate that PRE1 promotes the activation activity of ACE1 by inhibiting the negative activity of IBH1 on ACE1. PRE1 likely accomplishes this by interaction with IBH1, but not by interaction with ACE1. The final result of this double inhibition is increased expression of genes regulated by ACE1 and the promotion of cell elongation.

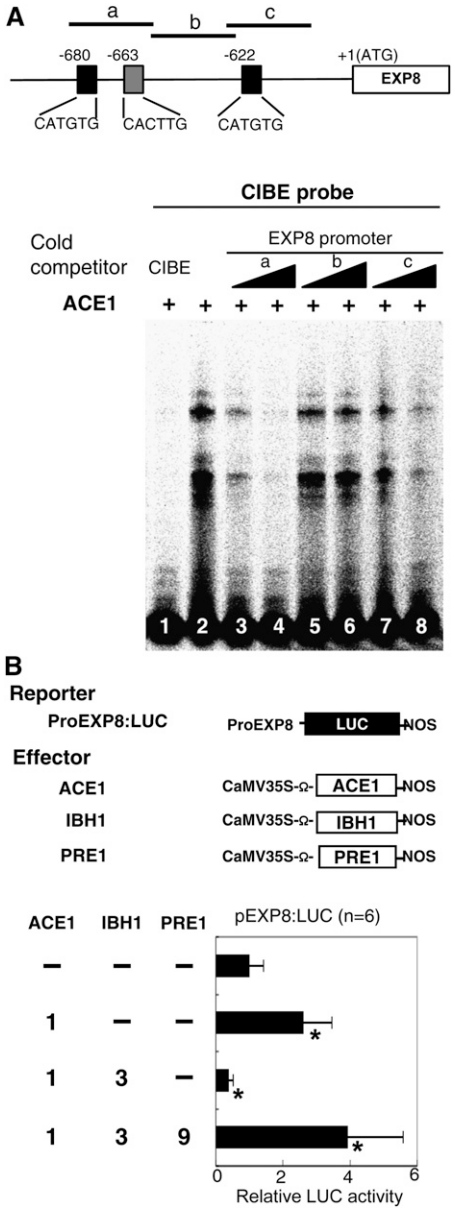

Figure 8. Analysis of Regulation of the Promoter Activity of *EXP8* by ACE1, IBH1, and PRE1.

(A) EMSA analysis of binding of ACE1 to the promoter of *EXP8*. Top panel: Gene structure of *EXP8.* The open box shows the coding region of *EXP8*, black line shows the 5′ upstream region of *EXP8*, and black and gray boxes show G-box–like motifs. Regions used as competitors are shown by short lines marked with letters (a, b, and c). Bottom panel: EMSA analysis using CIBE fragment as a probe, ACE1 as a protein, and portions of *EXP8* promoter as competitors. The CIBE probe was incubated with ACE1 protein. Unlabeled CIBE (lane 1) and portions of the promoter region of *EXP8* (lane 3 to 8) were used as competitor DNAs.
(B) Transient assay using *ProEXP8*:*LUC* reporter gene. Top panel: Schematic representation of the constructs used in transient expression analysis. *ProEXP8*:*LUC* reporter gene contained ~3 kb of 5′ upstream region of the translation initiation site of *EXP8* fused upstream of *LUC* (black box) and effector constructs for IBH1, ACE1, and PRE1, driven by the CaMV 35S promoter are shown. Ω, translation enhancer sequence derived from *Tobacco mosaic virus*. Bottom panel: Relative luciferase activities after cobombardment of *Arabidopsis* leaves with ACE1, IBH1, and PRE1 effectors, respectively, and the *ProEXP8*:*LUC* reporter gene. The relative activity due to vector control (top bar) was set as 1. Error bars indicate SD (n = 6). Asterisks indicate P values below 0.05 between vector control and others. Numbers indicate the ratio of effector construct (1 = 0.3 μg for one experiment).

Two Inhibitors, IBH1 and PRE1, and One Activator, ACE1, Regulate the Expression of *EXP8*

qRT-PCR analyses revealed that the expression of *EXP8* was decreased in *Pro35S*:*IBH1-SRDX* plants and *Pro35S*:*IBH1* plants, but it was increased in *ProIBH1*:*IBH1RNAi* plants (Figures 1L and 2G; see Supplemental Figure 3 online). To confirm whether IBH1, ACEs, and PRE1 directly regulate the expression of *EXP8*, we examined the direct binding of ACE1 to the promoter region of *EXP8* by EMSA. Competition EMSA showed that the short fragments of *EXP8* promoter that contain the G-box–like motif (fragments a and c) diminished the binding of ACE1 to CIBE fragment, but the fragment that did not contain a G-box–like element (fragment b) did not compete (Figure 8A). Therefore, these data showed specific binding of ACE1 to the G-box–like elements located in the *EXP8* promoter region.

Next, we performed transient expression assays using a reporter gene in which 3 kb of the *EXP8* 5′ upstream region was placed upstream of the LUC reporter gene (*ProEXP8*:*LUC*) (Figure 8B). Transient expression assays showed that the activity of *ProEXP8*:*LUC* increased when the *Pro35S*:*ACE1* (ACE1) effector was coexpressed (Figure 8B), indicating that ACE1 directly activated the expression of *EXP8*. Similar to the *CIBE4*:*LUC* reporter gene, the activation activity of ACE1 on the *ProEXP8*:*LUC* reporter gene was suppressed when *Pro35S*:*IBH1* (IBH1) effector was coexpressed (Figure 8B). Moreover, the suppressive activity of IBH1 effector was inhibited and the *ProEXP8*:*LUC* reporter gene activity was restored when the *Pro35S*:*PRE1* effector was coexpressed (Figure 8B). These results indicate that the expression of *EXP8* is likely to be regulated by a triple bHLH system, which is composed of one typical bHLH activator, ACE1, and two non-DNA binding HLH inhibitors, IBH1 and PRE1.

BR Controls Cell Elongation via Repression of IBH1 Expression

It was previously reported that *IBH1* expression is suppressed by BZR1 in BR signaling (Zhang et al., 2009). We confirmed that *IBH1* expression was suppressed by BL treatment and slightly increased in *det2* mutant plants, as shown previously (Figure 9A). By contrast, BL treatment did not affect the expression of either *ACE1*, *CIB5*, or *ACE2* (Figure 9A), indicating that the BR signaling cascade may not regulate the expression of *ACEs*.

Zhang et al. (2009) reported that BZR1 and its homolog BES1/BZR2 bound to the *IBH1* promoter and repressed its expression. Transient expression assays using a reporter gene in which the *IBH1* 5′-upstream region was placed upstream of the LUC gene (*ProIBH1*:*LUC*) showed that BZR1 and BES1 effectors (*Pro35S*:*BZR1* and *Pro35S*:*BES1*) suppressed the activity of the *ProIBH1*:

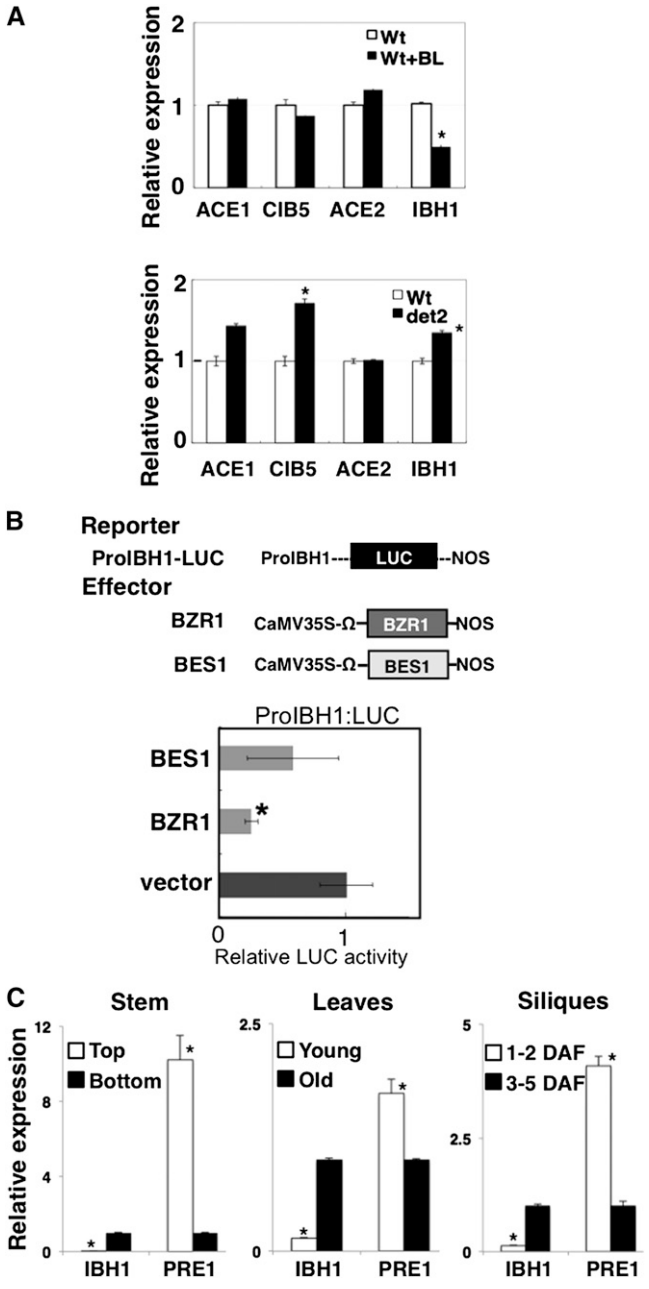

Figure 9. Analysis of *IBH1*, *ACEs*, *CIB5*, and *PRE1* Expression.

(A) The expression of the *ACE1*, *CIB5*, *ACE2*, and *IBH1* genes analyzed by qRT-PCR in wild-type (Wt) plants with or without 10^{-7} M BL treatment 4 h (top panel) and the wild type and *det2* mutant (bottom panel). The level of expression of the gene for ubiquitin was used for normalization of the results; for each gene, the expression level in wild-type plants without BL treatment was taken as 1. Asterisks indicate P values below 0.001 between the wild-type control and others.

(B) Analysis of regulation of the promoter activity of *IBH1* by BZR1 and BES1. Top panel: Schematic representation of the constructs used in the transient expression analysis. *ProIBH1*:*LUC* reporter gene contained 2353 bp 5′ upstream region of *IBH1* from the first ATG codon fused with the 5′ upstream of the LUC gene (black box), and the effectors for BZR1 (dark gray box) and BES1 (light gray box), driven by the CaMV 35S promoter are shown. Ω, translation enhancer sequence derived from *Tobacco mosaic virus*. Bottom panel: Relative luciferase activities after cobombardment of *Arabidopsis* leaves with BZR1 and BES1 effectors and the *ProIBH1*:*LUC* reporter gene. The relative activity due to vector control was set as 1. Error bars indicate SD (n = 3). Asterisks indicate P values below 0.05 between vector control and others.

(C) qRT-PCR analysis of the expression of the *IBH1* and *PRE1* genes in the top and bottom part of stem, young and old leaves, and young short siliques (1 to 2 d after flowering [DAF]) and elongated siliques (3 to 5 d after flowering). The level of expression of the gene for ubiquitin was used for normalization of the results; for each gene, the expression level in the bottom part of the stem, old leaves, and 3 to 5 d after flowering silique was taken as 1. Asterisks indicate P values below 0.02 between expression values for the bottom part of the stem, old leaves, and 3 to 5 d after flowering siliques and the other counterpart tissues.

LUC reporter gene, although the repressive activity of the BES1 effector was weaker than the BZR1 effector (Figure 9B). These results suggest that BR induces cell elongation via BZR1 repression of *IBH1* expression.

Expression of *PRE1*, *IBH1*, and *ACE*s during Development

To analyze the relationship between the expression patterns of *PRE1*, *IBH1*, and *ACEs* and the plant cell elongation during development, we performed qRT-PCR analysis using RNA isolated from stems, siliques, and leaves in cell-elongating and growth-arrested phases. *IBH1* expression levels were higher in the organs in growth-arrested phases, namely, the bottom parts of stems, and fully expanded old leaves and long siliques, where cell elongation was arrested, than in the organs in growth phase, namely, the top part of stems, young and small leaves, and short siliques (Figure 9C). By contrast, the expression of *PRE1* was essentially opposite to that of *IBH1*. For example, the expression of *PRE1* was higher in the organs in elongating phase tissues than in growth-arrested phase tissues (Figure 9C). These expression patterns of *IBH1* and *PRE1* in stem, leaves, and siliques were correlated with cell elongation and might be regulated by developmental factor(s). By contrast, the expression pattern of *ACEs* and *CIB5* do not appear to be correlated to growth phase nor to *IBH1* (see Supplemental Figure 7 online).

DISCUSSION

A Triantagonistic bHLH System Regulates Cell Elongation in *Arabidopsis* Development

Multiple endogenous phytohormones and environmental conditions regulate cell elongation in *Arabidopsis*. GA and BR play central roles in the positive regulation of cell elongation (Depuydt and Hardtke, 2011). *Arabidopsis* PRE1 promotes cell elongation regulated by GA and BR signaling (Lee et al., 2006; Zhang et al., 2009). IBH1, which was isolated as a PRE1 interactor, suppresses cell elongation under the control of BR signaling (Zhang et al., 2009). Ectopically expressed *IBH1* induces dwarfism, which can be suppressed by expression of *PRE1* (Zhang et al.,

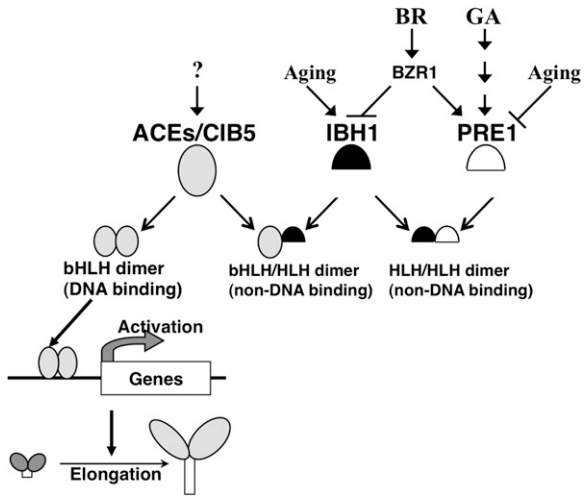

Figure 10. Summary of the Triantagonistic bHLH System That Regulates Cell Elongation in *Arabidopsis*.

PRE1 (open semicircle), IBH1 (black semicircle), and ACE/CIB5 (gray ovals) constitute a triantagonistic bHLH system that regulates cell elongation in *Arabidopsis*. ACE proteins form dimers, which can bind to the promoter *cis*-element and activate the transcription of genes required for cell elongation. IBH1 inhibits cell elongation by interfering with the formation of the ACEs DNA binding complex by forming heterodimers with the ACEs. PRE1 positively regulates cell elongation by recovering the activity of ACEs; to do this, PRE1 suppresses the inhibitory activity of IBH1 by forming heterodimers with IBH1. The expression levels of *IBH1* and *PRE1* are regulated by BR, GA, and developmental phase (aging).

2009). In this report, we demonstrated the mechanisms by which IBH1 negatively and PRE1 positively regulate the elongation of plant cells.

We found that IBH1 acts as a transcriptional repressor, but it does not have an active repressive activity (Figures 1, 2, and 4). IBH1 interacts with other typical bHLHs (ACEs and CIB5), which act as transcriptional activators for cell elongation (Figure 5), and interferes with their transcriptional activation activities (Figure 6). IBH1 does not bind to the G-box (Figure 6E), likely because it lacks important amino acids necessary for G-box and E-box binding (see Supplemental Figure 4 online), indicating that it does not act by competing for a *cis*-activation site. Rather, it is likely that IBH1 inhibits the CIBE binding activity of ACEs through the formation of a heterodimer; a similar mechanism has been shown for the human Id-1 protein (Ruzinova and Benezra, 2003). We also revealed that PRE1 interferes with the inhibitory activity of IBH1 by forming a heterodimer with IBH1 (Figures 6 to 8).

We demonstrated here that cell elongation in *Arabidopsis* is regulated by a system that we call a triantagonistic bHLH system, which is composed of a group of typical bHLH transcriptional activators, ACEs and CIB5, and two atypical HLH inhibitors, IBH1 and PRE1. In Figure 10, we summarize this triantagonistic bHLH regulation system for cell elongation. The bHLH transcriptional activators, ACEs and CIB5, positively regulate cell elongation by direct activation of the expression of the genes related for cell elongation, including *EXP8* (Figure 8). IBH1 negatively regulates cell elongation by forming heterodimers with ACEs and thus suppressing their G-box binding activity. PRE1 positively regulates cell elongation by forming heterodimers with IBH1 and thus suppressing IBH1 inhibition of the ACEs (Figure 10).

In this system, the balance of ACEs, IBH1, and PRE1 proteins regulates cell elongation. The activation activity of ACEs is regulated by the heterodimerization between ACEs and IBH1, and PRE1 and IBH1, respectively. PRE1 is known to be one of the key factors that regulate cell elongation under GA signaling (Lee et al., 2006). The ectopic expression of *PRE1* promotes cell elongation even though the endogenous GA concentration is low, suggesting that GA promotes cell elongation by inducing the expression of *PRE1* (Lee et al., 2006; Zhang et al., 2009). PRE1 induced by GA promotes cell elongation by interfering with the interaction of IBH1 with ACEs under the triantagonistic bHLH system. By contrast, BR promotes cell elongation probably by repressing the expression of *IBH1* by BZR1 because ectopic expression of *IBH1* induces a BR-insensitive phenotype (Figure 2; Zhang et al., 2009). The downregulation of *IBH1* would promote the activity of ACEs probably through enhancement of ACE DNA binding activity, resulting in induction of cell elongation via activation of the expression of enzymatic genes related to cell elongation. The GA and BR signals for cell elongation might be integrated by this triantagonistic bHLH system.

The expression patterns of *IBH1* and *PRE1* suggest that the expression of these genes is also regulated by growth phase–dependent factors (Figure 9C). Although the expression of *ACE*s does not always correlate with growth phase, the highly expressed *PRE1* in tissues of growth phase could suppress the inhibitory activity of IBH1 by forming a heterodimer with it and enhancing the transcriptional activation activity of ACEs in growth-phase elongating tissues. By contrast, in growth arrest phase tissues, highly expressed *IBH1* could inhibit activity of ACEs by interacting with them. The cell elongation phase–dependent signal(s) also may be integrated in this triantagonistic bHLH system.

In this report, the expression of *ACEs* and *CIB5* does not appear to be clearly correlated with BR or cell elongation phase (Figure 9A; see Supplemental Figure 7 online). Each ACE protein might act under different signaling pathways even though each ACE acts as a positive regulator of cell elongation. Although the activities of ACE proteins are regulated by heterodimerization with IBH1, the expression pattern could also be important for the regulation of cell elongation. In future work, detailed analysis of the regulation of the expression of each *ACE* will be important.

In plants, regulation of cell elongation is pivotal for normal development and for adaptation to changing environmental conditions. We show here that some signals, including BR, GA, and growth phase–dependent factors, might regulate cell elongation via the triantagonistic bHLH system composed of ACEs, IBH1, and PRE1. Further studies of the triantagonistic bHLH systems will provide more information on plant development and environmental adaptation.

METHODS

Construction of Plasmids

The coding regions and the 5′-upstream regions of genes used in this study were amplified from a cDNA library or from *Arabidopsis thaliana* genomic DNA with the appropriate primers (see Supplemental Table 3 online). Constructs for overexpression, CRES-T, VP16 fusion, GFP fusion, and Flag fusion, of each gene were based on modified vectors derived from pGreenII0029 (Hellens et al., 2000), p35SSRDXG (Mitsuda et al., 2006), p35SVP16 (Triezenberg et al., 1988), p35SGFP, and pGWB11 (Nakagawa et al., 2007). Preparation of the cDNA library and bait construct for Y2H screening was described previously (Mitsuda et al., 2010). Construction of the effectors and reporter plasmids for transient expression assays was also described previously (Hiratsu et al., 2002). Effector plasmids fused with Gal4 DNA binding domain (Gal4DB) were constructed by fusion of the yeast Gal4DB-coding region to the coding sequence of each gene, in frame, under the control of the CaMV 35S promoter (−800 to +8). The reporter gene *35S-Gal4-TATA-LUC-NOS* was described previously (Hiratsu et al., 2002). Synthetic sense and antisense DNAs of CIBE (see Supplemental Table 3 online; Liu et al., 2008) were annealed and introduced into the *p190LUC* vector (Fujimoto et al., 2000; Mitsuda et al., 2010) using the appropriate restriction enzyme and used as CIBEx4 constructs. The 5′ upstream region of 2352 bp, which extended from the site of initiation of translation of the *Arabidopsis IBH1* gene and 2714 bp, which extended from the site of initiation of translation of the *Arabidopsis EXP8* gene, were used for preparation of the *ProIBH1:LUC* and *ProEXP8:LUC* reporter constructs, respectively. The 2352-bp 5′ upstream sequence of *IBH1* was cloned into pHG8_pro-less, in which the 35S promoter and *NPTII* gene of pHellsgate8 (Helliwell and Waterhouse, 2003) are substituted into the multicloning site and *HPT* gene, respectively. The coding sequence of *IBH1* was transferred into this vector by Gateway reaction to prepare *ProIBH1:IBH1RNAi*. Constructs for protein production used the pMAL-c2 (NEB) vector. cDNA fragments fused with the Flag tag were amplified by appropriate primer sets (see Supplemental Table 3 online), digested with *Sal*I and *Hin*dIII and cloned into pMAL-c2.

Growth and Transformation of Plants

Arabidopsis Columbia-0 was used in all experiments. Plants used for transient expression assays and for transformation were grown in soil at 23°C with a photoperiod of 10 h/14 h and 16 h/8 h light/dark, respectively. Transformation of *Arabidopsis* was performed using the floral dip method (Clough and Bent, 1998). Seedlings used for RNA isolation were grown on agar plates or on soil at 23°C with a photoperiod of 16 h/8 h light/dark.

Microscopy

Plant tissues were rendered transparent as described previously (Aida et al., 1997). Observations were performed using the Axioskop2 Plus system (Carl Zeiss). For scanning electron microscopy, fresh samples were observed using a scanning electron microscope (real 3D system model VE8800; Keyence) at an accelerating voltage of 1 or 2 kV.

BL Treatment and Measurement of Organ Length

For measurement of the length of hypocotyls and cotyledons, 7-d-old seedlings were grown on agar plates containing Gamborg's B5 medium at 23°C with a photoperiod of 16 h/8 h light/dark. For measurement of the length of hypocotyls and cotyledons with and without BL treatment, 5-d-old seedlings were transferred into liquid Gamborg's B5 medium containing appropriate concentrations of BL and incubated for 3 d at 23°C with a photoperiod of 16 h/8 h light/dark. For total RNA isolation from BL-treated plants, 10-d-old seedlings grown on agar plates were transferred into liquid Gamborg's B5 medium containing the appropriate concentration of BL and incubated for 4 h at 23°C under light conditions.

Fluorescence Observation

BiFC assays were performed as described previously (Bracha-Drori et al., 2004; Walter et al., 2004). For BiFC assays, NSC and C2 vectors were constructed by insertion of the coding sequences for amino acids 1 to 154 and 155 to 239 of enhanced yellow fluorescent protein, respectively, into the Aor51HI site of the pUGW2 vector (Nakagawa et al., 2007). Coding sequences of the *IBH1*, *PRE1*, and *ACE* genes without the stop codon were amplified by primer pairs with an *att*B1/B2 site (see Supplemental Table 3 online) and cloned into the pDONR207 vector (Life Technologies) by BP cloning. Cloned coding sequences were transferred into NSC or C2 vectors by LR clonase. The 35S-driven monomeric red fluorescent protein–fused *VAM3* whose gene product localizes to the vacuolar membrane (Uemura et al., 2010) was used as a control. The fluorescence of yellow fluorescent protein and GFP was visualized after bombardment, and all observations by light and fluorescence microscopy were done with the Axioskop2 Plus system (Carl Zeiss).

Transient Expression Assays

Transient expression assays were performed using expanded *Arabidopsis* leaves of 2-month old plants, as described previously (Hiratsu et al., 2004). After particle bombardment, the *Arabidopsis* leaves were incubated at 23°C under continuous dark conditions.

Isolation of RNA and Analysis of RNA Expression

Total RNA was isolated using the RNeasy plant mini kit (Qiagen), from more than 10 individual plants. After treatment with DNase I, cDNAs were prepared using the PrimeScript RT reagent kit (Perfect Real Time; Takara-Bio). qRT-PCR was performed by the SYBR green method using the ABI 7300 real-time PCR system (Life Technologies) with the appropriate primers (see Supplemental Table 3 online). To quantify relative expression of each gene in each sample, the standard curve was prepared by plotting the cycle threshold value for a series of four dilutions of the standard sample in which all the cDNA samples were mixed. All standard curves described in this study are shown in Supplemental Figure 8 online. The cycle threshold value for each sample was automatically calculated by the software provided by the manufacturer. The relative level of transcript in each sample to the standard sample was calculated using the standard curve. The expression of each transcript was normalized against the amount of *Ubiquitin1* control transcripts in each sample. More than three replicates were included in each experiment. Results are presented as the mean ± SD. The absence of an error bar indicates that the bar falls within the symbol. All statistical tests were performed by two-sided Welch's *t* test in this study.

Y2H Screening

The Y2H assays were performed as described previously (Mitsuda et al., 2010). For bait construction, *IBH1*cDNAs with the stop codon were amplified by a pair of primers with an *att*B1/B2 site (see Supplemental Figure 3 online) and cloned into the pDONR207 vector (Life Technologies) by BP cloning. Cloned cDNAs were transferred into pDEST_BTM116 by LR clonase.

Microarray Analysis

The microarray experiments were performed using the Agilent *Arabidopsis* 3 (44k) microarray (Agilent Technologies) according to the manufacturer's instructions. Three biological replicates were tested with a

two-color method in which wild-type RNA was labeled by Cy3 in two replicates and labeled by Cy5 in one replicate. Spot signal values were calculated by Feature Extraction version 9.1 software supplied by Agilent, and this step includes dye normalization by the Lowess method (Cleveland, 1981). We defined QC value as 1 when a spot passed the FeatNonUnifOL filter and as 2 when the spot further passed the FeatPopnOL filter. We defined detection value as 1 when a spot passed the IsPosAndSignif filter and as 2 when the spot further passed the IsWellAboveBG filter. All signal values were divided by the median value among spots with QC = 2 to make it possible to compare with other microarray data. Spot-to-gene conversion was accomplished based on a table provided by The Arabidopsis Information Resource (ftp://ftp.Arabidopsis.org/home/tair/Microarrays/Agilent/agilent_array_elements-2010-12-20.txt). The average values were used in the genes corresponding to two or more probes. All data was uploaded to the National Center for Biotechnology Information Gene Expression Omnibus (http://www.ncbi.nlm.nih.gov/geo/; GSE35098).

EMSAs

Proteins were synthesized and purified using the pMAL system (NEB). IRDye-labeled synthetic oligonucleotide (GWTf; LI-COR) was annealed with GWTr oligonucleotide (see Supplemental Table 3 online) and was used for DNA probe. A DNA-protein binding reaction was performed using the Odyssey infrared EMSA kit (LI-COR). The reaction contains 0.5 ng DNA, 10 mM Tris, 50 mM KCl, 3.5 mM DTT, 0.25% Tween 20, 1 μg poly dI-dC, and 5% glycerol as well as the indicated amount of unlabeled competitor or protein. The reactions were incubated at room temperature for 20 min under dark conditions and fractioned by electrophoresis in a 5% native polyacrylamide gel containing 2.5% glycerol and Tris-borate-EDTA buffer. The signals were detected by Odyssey infrared imaging system (LI-COR).

In Vivo Protein–Protein Interaction Assay

Transient protein coexpression using *Nicotiana benthamiana* and coimmunoprecipitation was performed as described previously (Kim et al., 2007). The immunoprecipitates were separated by SDS-PAGE (e-PAGEL; Atto) and transferred to Polyvinylidene difluoride (PVDF) membrane (Bio-Rad). The blots were incubated with anti-GFP antibody (1:2500; Abcam) or anti-DYKDDDDK-HRP (1:15,000; Wako) and detected by ECL plus (GE healthcare).

Accession Numbers

Sequence data from this article can be found in the Arabidopsis Genome Initiative or GenBank/EMBL databases under the following accession numbers: IBH1 (At2g43060), PRE1 (At5g39860), PRE2 (At5g15160), PRE3 (At1g74500), PRE4 (At3g47710), PRE5 (At3g28857), PRE6 (At1g26945), ACE1 (At1g68920), ACE2 (At1g10120), ACE3 (At3g23690), CIB1 (At4g34530), CIB5 (At1g26260), bHLH137 (At5g50915), AIF1 (At3g05800), AIF2 (At3g06590), AIF3 (At3g17100), AIF4 (At1g09250), EXP8 (At2g40610), XTH4 (At2g06850), EXPL2 (At4g38400), UBQ (At3g52590), BZR1 (At1g75080), and BES1 (At1g19350).

Supplemental Data

The following materials are available in the online version of this article.

Supplemental Figure 1. Morphological Analyses of *Pro35S*:*IBH1-SRDX* Plants.

Supplemental Figure 2. The Level of the Expression of *IBH1* in *Pro35S*:*IBH1* (IBH1ox) Seedlings.

Supplemental Figure 3. The Expression of the *IBH1* and *EXP8* in *ProIBH1*:*IBH1RNAi* Plants.

Supplemental Figure 4. An Alignment of Amino Acid Sequences of IBH1 and Related Proteins.

Supplemental Figure 5. Phylogenetic Tree of a Subset of *Arabidopsis* bHLH Transcription Factors.

Supplemental Figure 6. BiFC Assay in Epidermal Cells of Onion.

Supplemental Figure 7. qRT-PCR Analysis for the Expression of the *ACEs* and *CIB5*.

Supplemental Figure 8. Standard Curves for Each qRT-PCR Experiment.

Supplemental Table 1. The Fold Change of Expression of Genes for EXPANSIN and XYLOGLUCAN ENDO-TRANSGLYCOSYLASE/HYDROLASE in *Pro35S*:*IBH1SRDX* Plants and Three Other Experiments.

Supplemental Table 2. TFs That Interact with IBH1, as Identified by Yeast Two-Hybrid Screening.

Supplemental Table 3. Oligonucleotides Used in This Study.

Supplemental Data Set 1. Text File of Alignment Used for Phylogenetic Tree in Supplemental Figure 5.

ACKNOWLEDGMENTS

We thank Eimi Ito and Takashi Ueda (University of Tokyo) for the NSC and C2 vectors and Tomohiro Uemura (University of Tokyo) for the 35S-driven monomeric red fluorescent protein–fused *VAM3* plasmid. We also thank Yoko Ooi, Fumie Tobe, Yuko Takiguchi, and Miyoko Yamada for their skilled technical assistance as well as Sumiko Takahashi and Yoshimi Sugimoto (National Institute of Advanced Industrial Science and Technology) for cultivation of plants. This work was partially supported by a Grant-in-Aid for Japanese Society for the Promotion of Science Restart Postdoctoral Fellowships.

AUTHOR CONTRIBUTIONS

M.I. designed the research. M.I., S.F., and N.M. performed research and analyzed data. N.M. performed microarray experiment and analyzed the microarray data. M.I., S.F., N.M. and M.O.-T. wrote the article. M.O.-T. supervised the overall project.

Received September 10, 2012; revised October 9, 2012; accepted October 25, 2012; published November 29, 2012.

REFERENCES

Aida, M., Ishida, T., Fukaki, H., Fujisawa, H., and Tasaka, M. (1997). Genes involved in organ separation in *Arabidopsis*: An analysis of the cup-shaped cotyledon mutant. Plant Cell **9:** 841–857.

Bracha-Drori, K., Shichrur, K., Katz, A., Oliva, M., Angelovici, R., Yalovsky, S., and Ohad, N. (2004). Detection of protein-protein interactions in plants using bimolecular fluorescence complementation. Plant J. **40:** 419–427.

Briggs, W.R., and Huala, E. (1999). Blue-light photoreceptors in higher plants. Annu. Rev. Cell Dev. Biol. **15:** 33–62.

Cleveland, W.S. (1981). LOWESS: A program for smoothing scatterplots by robust locally weighted regression. Am. Stat. **35:** 54.

Clough, S.J., and Bent, A.F. (1998). Floral dip: A simplified method for Agrobacterium-mediated transformation of *Arabidopsis thaliana*. Plant J. **16:** 735–743.

Clouse, S.D. (2011). Brassinosteroid signal transduction: from receptor kinase activation to transcriptional networks regulating plant development. Plant Cell **23:** 1219–1230.

Clouse, S.D., Langford, M., and McMorris, T.C. (1996). A brassinosteroid-insensitive mutant in *Arabidopsis thaliana* exhibits multiple defects in growth and development. Plant Physiol. **111:** 671–678.

Depuydt, S., and Hardtke, C.S. (2011). Hormone signalling crosstalk in plant growth regulation. Curr. Biol. **21:** R365–R373.

Fujimoto, S.Y., Ohta, M., Usui, A., Shinshi, H., and Ohme-Takagi, M. (2000). *Arabidopsis* ethylene-responsive element binding factors act as transcriptional activators or repressors of GCC box-mediated gene expression. Plant Cell **12:** 393–404.

Heim, M.A., Jakoby, M., Werber, M., Martin, C., Weisshaar, B., and Bailey, P.C. (2003). The basic helix-loop-helix transcription factor family in plants: A genome-wide study of protein structure and functional diversity. Mol. Biol. Evol. **20:** 735–747.

Hellens, R.P., Edwards, E.A., Leyland, N.R., Bean, S., and Mullineaux, P.M. (2000). pGreen: A versatile and flexible binary Ti vector for Agrobacterium-mediated plant transformation. Plant Mol. Biol. **42:** 819–832.

Helliwell, C., and Waterhouse, P. (2003). Constructs and methods for high-throughput gene silencing in plants. Methods **30:** 289–295.

Hiratsu, K., Matsui, K., Koyama, T., and Ohme-Takagi, M. (2003). Dominant repression of target genes by chimeric repressors that include the EAR motif, a repression domain, in *Arabidopsis*. Plant J. **34:** 733–739.

Hiratsu, K., Mitsuda, N., Matsui, K., and Ohme-Takagi, M. (2004). Identification of the minimal repression domain of SUPERMAN shows that the DLELRL hexapeptide is both necessary and sufficient for repression of transcription in *Arabidopsis*. Biochem. Biophys. Res. Commun. **321:** 172–178.

Hiratsu, K., Ohta, M., Matsui, K., and Ohme-Takagi, M. (2002). The SUPERMAN protein is an active repressor whose carboxy-terminal repression domain is required for the development of normal flowers. FEBS Lett. **514:** 351–354.

Hyun, Y., and Lee, I. (2006). KIDARI, encoding a non-DNA Binding bHLH protein, represses light signal transduction in *Arabidopsis thaliana*. Plant Mol. Biol. **61:** 283–296.

Ikeda, M., Mitsuda, N., and Ohme-Takagi, M. (2009). *Arabidopsis* WUSCHEL is a bifunctional transcription factor that acts as a repressor in stem cell regulation and as an activator in floral patterning. Plant Cell **21:** 3493–3505.

Ikeda, M., and Ohme-Takagi, M. (2009). A novel group of transcriptional repressors in *Arabidopsis*. Plant Cell Physiol. **50:** 970–975.

Kim, W.Y., Fujiwara, S., Suh, S.S., Kim, J., Kim, Y., Han, L., David, K., Putterill, J., Nam, H.G., and Somers, D.E. (2007). ZEITLUPE is a circadian photoreceptor stabilized by GIGANTEA in blue light. Nature **449:** 356–360.

Lee, S., Lee, S., Yang, K.Y., Kim, Y.M., Park, S.Y., Kim, S.Y., and Soh, M.S. (2006). Overexpression of PRE1 and its homologous genes activates Gibberellin-dependent responses in *Arabidopsis thaliana*. Plant Cell Physiol. **47:** 591–600.

Li, J. (2005). Brassinosteroid signaling: From receptor kinases to transcription factors. Curr. Opin. Plant Biol. **8:** 526–531.

Li, J., and Chory, J. (1997). A putative leucine-rich repeat receptor kinase involved in brassinosteroid signal transduction. Cell **90:** 929–938.

Li, Y., Jones, L., and McQueen-Mason, S. (2003). Expansins and cell growth. Curr. Opin. Plant Biol. **6:** 603–610.

Liu, H., Yu, X., Li, K., Klejnot, J., Yang, H., Lisiero, D., and Lin, C. (2008). Photoexcited CRY2 interacts with CIB1 to regulate transcription and floral initiation in *Arabidopsis*. Science **322:** 1535–1539.

Mitsuda, N., Hiratsu, K., Todaka, D., Nakashima, K., Yamaguchi-Shinozaki, K., and Ohme-Takagi, M. (2006). Efficient production of male and female sterile plants by expression of a chimeric repressor in *Arabidopsis* and rice. Plant Biotechnol. J. **4:** 325–332.

Mitsuda, N., Ikeda, M., Takada, S., Takiguchi, Y., Kondou, Y., Yoshizumi, T., Fujita, M., Shinozaki, K., Matsui, M., and Ohme-Takagi, M. (2010). Efficient yeast one-/two-hybrid screening using a library composed only of transcription factors in *Arabidopsis thaliana*. Plant Cell Physiol. **51:** 2145–2151.

Nakagawa, T., et al. (2007). Improved Gateway binary vectors: high-performance vectors for creation of fusion constructs in transgenic analysis of plants. Biosci. Biotechnol. Biochem. **71:** 2095–2100.

Ohta, M., Matsui, K., Hiratsu, K., Shinshi, H., and Ohme-Takagi, M. (2001). Repression domains of class II ERF transcriptional repressors share an essential motif for active repression. Plant Cell **13:** 1959–1968.

Rose, J.K., Braam, J., Fry, S.C., and Nishitani, K. (2002). The XTH family of enzymes involved in xyloglucan endotransglucosylation and endohydrolysis: Current perspectives and a new unifying nomenclature. Plant Cell Physiol. **43:** 1421–1435.

Ruzinova, M.B., and Benezra, R. (2003). Id proteins in development, cell cycle and cancer. Trends Cell Biol. **13:** 410–418.

Stamm, P., and Kumar, P.P. (2010). The phytohormone signal network regulating elongation growth during shade avoidance. J. Exp. Bot. **61:** 2889–2903.

Sun, Y., et al. (2010). Integration of brassinosteroid signal transduction with the transcription network for plant growth regulation in *Arabidopsis*. Dev. Cell **19:** 765–777.

Toledo-Ortiz, G., Huq, E., and Quail, P.H. (2003). The *Arabidopsis* basic/helix-loop-helix transcription factor family. Plant Cell **15:** 1749–1770.

Triezenberg, S.J., Kingsbury, R.C., and McKnight, S.L. (1988). Functional dissection of VP16, the trans-activator of herpes simplex virus immediate early gene expression. Genes Dev. **2:** 718–729.

Uemura, T., Morita, M.T., Ebine, K., Okatani, Y., Yano, D., Saito, C., Ueda, T., and Nakano, A. (2010). Vacuolar/pre-vacuolar compartment Qa-SNAREs VAM3/SYP22 and PEP12/SYP21 have interchangeable functions in *Arabidopsis*. Plant J. **64:** 864–873.

Walter, M., Chaban, C., Schütze, K., Batistic, O., Weckermann, K., Näke, C., Blazevic, D., Grefen, C., Schumacher, K., Oecking, C., Harter, K., and Kudla, J. (2004). Visualization of protein interactions in living plant cells using bimolecular fluorescence complementation. Plant J. **40:** 428–438.

Wang, H., Zhu, Y., Fujioka, S., Asami, T., Li, J., and Li, J. (2009). Regulation of *Arabidopsis* brassinosteroid signaling by atypical basic helix-loop-helix proteins. Plant Cell **21:** 3781–3791.

Yu, X., Li, L., Zola, J., Aluru, M., Ye, H., Foudree, A., Guo, H., Anderson, S., Aluru, S., Liu, P., Rodermel, S., and Yin, Y. (2011). A brassinosteroid transcriptional network revealed by genome-wide identification of BES1 target genes in *Arabidopsis thaliana*. Plant J. **65:** 634–646.

Zhang, L.Y., et al. (2009). Antagonistic HLH/bHLH transcription factors mediate brassinosteroid regulation of cell elongation and plant development in rice and *Arabidopsis*. Plant Cell **21:** 3767–3780.